CRATER SCALING ON WEAK TARGETS, FROM CERES TO ICY SATELLITES. N. Schmedemann[1], R. J. Wagner[4], G. Michael[1], B. A. Ivanov[2], T. Kneissl[1], A. Neesemann[1], H. Hiesinger[3], R. Jaumann[1,4], C. A. Raymond[5], C. T. Russell[6], [1]Institute of Geological Sciences, Freie Universität Berlin, Berlin, Germany, [2]Institute of Dynamics of Geospheres, Moscow, Russia, [3]Institut für Planetologie, Westfälische Wilhelms-Universität, Münster, Germany, [4]German Aerospace Center, Institute of Planetary Research, Berlin, Germany, [5]JPL, Caltech, Pasadena, CA, USA, [6]University of California, Los Angeles, CA, USA. (nico.schmedemann@fu-berlin.de)

Introduction: The highly successful Dawn mission [1] finished data collection at Vesta in 2012, went into orbit about Ceres in March 2015 and began to acquire high resolution imaging data from its **L**ow **A**ltitude **M**apping **O**rbit (LAMO) in December 2015. In our LPSC abstract last year [2] we proposed a preliminary lunar-derived chronology for Ceres on a theoretical basis. Analysis of the crater size-frequency distribution (CSFD) from higher resolution imaging data obtained during the Survey orbit, High Altitude Mapping Orbit (HAMO) as well as Low Altitude Mapping Orbit (LAMO) shows high consistency with that crater production function (PF) of [2] (Fig.1).

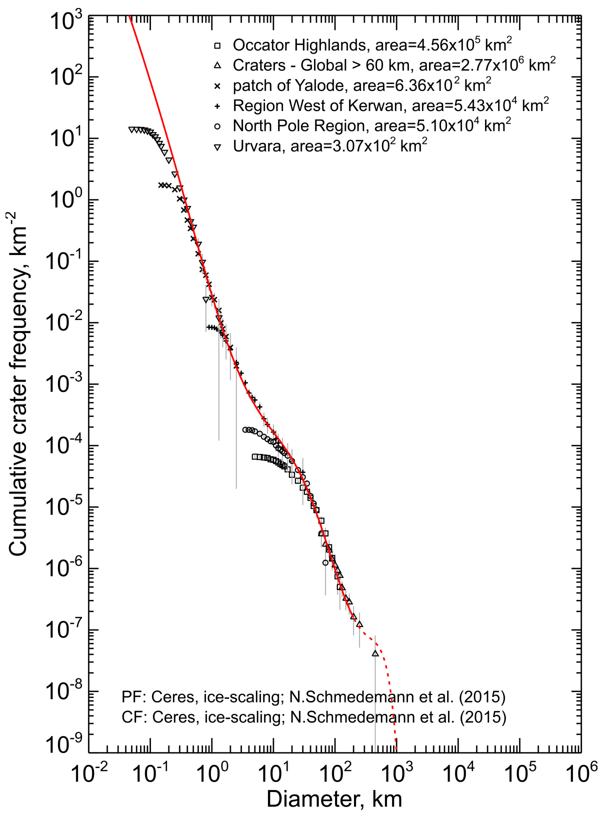

Fig. 1: Vertically normalized CSFD of six different measurement areas on Ceres in comparison with a theoretically derived PF [2].

The high content of volatile materials on Ceres [3] as well as the comparatively well known impact conditions (projectile source and impact velocity) make Ceres an important key to understanding the cratering records of icy satellites in the outer Solar System. Saturnian satellites are more similar in their target properties to Ceres than to basaltic bodies, such as the Moon or Vesta [2]. Ceres and Rhea were shown to be highly similar [4,5] in their target properties as well as their CSFDs, if only corrected for different exposure ages. In this work we derive the PF for the Jovian satellites Ganymede and Callisto based on scaling laws [6] and derivation techniques used for the Cerean PF [2]. The resulting PFs are compared with measured CSFDs in a complementary work presented by Wagner et al. at this conference.

Methodology: For scaling between crater sizes and projectile sizes on various bodies we use tentatively the Ivanov scaling laws for low friction low porocity materials (Eq 1) [6].

$$\frac{D_t}{D_P\left(\frac{\delta}{\rho}\right)^{0.43}(v\sin\alpha)^{0.55}} = \frac{1.21}{[(D_{sg}+D_t)g]^{0.28}} \quad (1)$$

D_t is the diameter of the transient crater and D_P is the diameter of the projectiles. For simple craters the transient crater diameter is nearly the same as the final crater diameter. [6] gives a second equation for computing the diameter of complex craters from the transient crater diameter. We plan more work to take into account more relevant scaling laws. Weak targets such as icy satellites show significantly smaller simple to complex crater transitions than stronger basaltic targets [6]. This can be accommodated within the scaling laws by using a modified surface gravity for the weak target bodies that corresponds to the surface gravity of strong target bodies at the same simple to complex transition crater diameter [2]. Table 1 gives the used parameters for Ceres, Ganymede and Callisto. With respect to [2] Ceres parameters in Table 1 are slightly changed based on observations during the Dawn at Ceres mission. The simple to complex transition diameters for Ganymede and Callisto are taken from [7], and impact velocities are taken from [8].

Table1: Scaling parameters for the Ceres, Ganymede and Callisto. Numbers in brackets give the modified surface gravity used with the scaling law. Impact velocities are given for heliocentric and planetocentric projectile trajectories.

Parameter	Ceres	Ganymede	Callisto
ρ; target density [g/cm³]	1.5	1	1
δ; projectile density [g/cm³]	2	2	2
v; impact velocity [km/s] (heliocentric)	4.6	20	15.7
v; impact velocity [km/s] (planetocentric)	-	5.76	4.52
α; impact angle [degree]	45	45	45
g; surface gravity [m/s²]	0.276 (1.75)	1.42 (13.5)	1.32 (12.79)
sg; strength-gravity trans. [km]	0.277	0.036	0.038
sc; simple-complex trans. [km]	10	1.8	1.9

Results: For the case of heliocentric projectiles the resulting coefficients for a polynomial of 11th degree are given in Table 2, and for planetocentric projectiles in Table 3.

Table 2: Coefficients for the polynomial function of 11th degree for Ceres, Ganymede and Callisto (heliocentric case).

	Ceres	Ganymede	Callisto
a_0	−3.197	−2.621	−2.772
a_1	−3.335	−3.684	−3.636
a_2	0.8333	0.9709	1.012
a_3	0.7512	0.8072	0.8246
a_4	−0.1603	−0.4082	−0.374
a_5	−0.3077	−0.2321	−0.2806
a_6	−1.502e-02	0.1976	0.1538
a_7	5.147e-02	−3.231e-02	8.599e-03
a_8	6.844e-03	−3.532e-02	−3.147e-02
a_9	−3.366e-03	2.182e-02	1.069e-02
a_{10}	−4.352e-04	−4.019e-03	−4.548e-04
a_{11}	4.392e-05	1.691e-04	−2.044e-04

Fig. 2 shows the respective PFs. The planetocentric cases for Ganymede and Callisto are nearly identical but are distinct from the heliocentric cases. Hence, the observed crater distributions may allow us to determinate the predominant projectile dynamics.

This is a preliminary work and several issues such as variable surface temperatures on the individual bodies have not yet been addressed.

Table 3: Coefficients for the polynomial function of 11th degree for Ganymede and Callisto (planetocentric case).

	Ganymede	Callisto
a_0	−3.449	−3.582
a_1	−3.257	−3.168
a_2	1.353	1.407
a_3	0.6811	0.6412
a_4	−0.5472	−0.5901
a_5	−0.3126	−0.3155
a_6	0.1657	0.1755
a_7	5.157e-02	5.527e-02
a_8	−3.841e-02	−4.002e-02
a_9	7.360e-04	4.439e-04
a_{10}	4.214e-03	4.469e-03
a_{11}	−8.623e-04	−9.180e-04

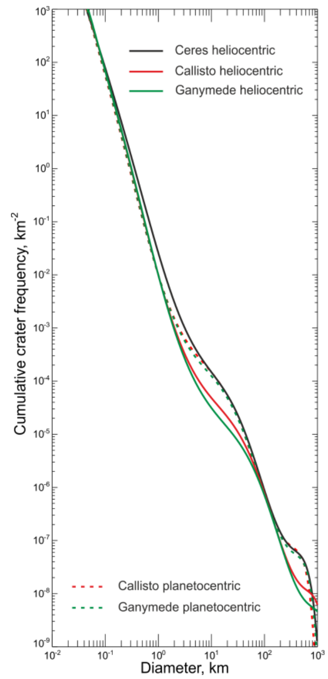

Fig. 2:PF vertically normalized at ~50 m diameter for Ceres, Ganymede and Callisto for the mentioned dynamical cases. The individual functions do not represent the same surface exposure age.

References: [1] Russell C.T. et al. (2012) Science, 336, 684-686. [2] Schmedemann N. et al. (2015) , LPSC XLVI, abstr. #1418. [3] Nathues A. et al. (2015) Nature, 528, 237–240. [4] Schmedemann N. et al. (2015), EPSC Abstracts, Vol. 10, abstr. EPSC2015-367. [5] Schmedemann N. et al. (2015), AGU Abstracts, P42A-07. [6] Ivanov, B., Size-Frequency Distribution Of Asteroids And Impact Craters: Estimates Of Impact Rate, in Catastrophic Events Caused by Cosmic Objects, edited by V. Adushkin, and I. Nemchinov, pp. 91-116, Springer Netherlands, 2008. [8] Neukum G. (1985) Adv. Space Res., 5, 107-116.

Acknowledgments: This work has been supported by the German Space Agency (DLR) on behalf of the Federal Ministry of Economic Affairs and Energy, grants 50OW1505 (NS, TK, AN) and 50QM1301 (GM). BAI is supported by Program 9 RAS.